

# Development of a Transcriptional Biosensor for Hydrogen Sulfide That Functions under Aerobic and Anaerobic Conditions

Matthew T. Fernandez, Shanthi Hegde, Justin A. Hayes, Kathryn O. Hoyt, Rebecca L. Carrier, and Benjamin M. Woolston\*



Cite This: *ACS Synth. Biol.* 2025, 14, 2198–2207



Read Online

ACCESS |

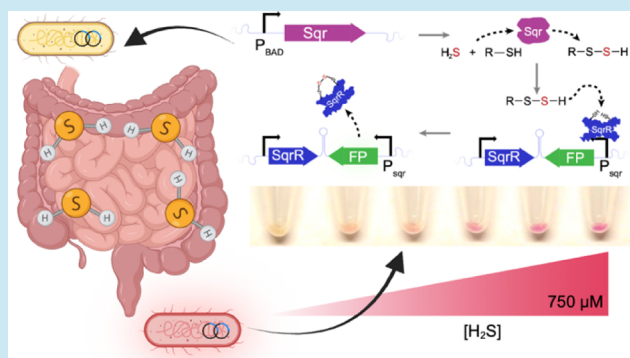
Metrics & More

Article Recommendations

Supporting Information

**ABSTRACT:** Hydrogen sulfide ( $\text{H}_2\text{S}$ ) is a gaseous gut metabolite with disputed effects on gastrointestinal health. Monitoring  $\text{H}_2\text{S}$  concentration in the gut would provide insight into its role in disease but is complicated by sulfide's reactivity and volatility. Here we develop a transcriptional sulfide biosensor in *Escherichiacoli*. The sensor relies on enzymatic oxidation of sulfide catalyzed by a sulfide:quinone oxidoreductase (Sqr) to polysulfides, which interact with the repressor SqrR, triggering unbinding from the promoter and transcription of the reporter. Through promoter engineering and improved soluble SqrR expression, we optimized the system to provide an operational range of 50–750  $\mu\text{M}$  and a dynamic range of 18 aerobically. To enable sensing in anaerobic environments, we identified an Sqr from *Wolinella succinogenes* that uses menaquinone, facilitating reoxidation through the anaerobic electron transport chain by fumarate or nitrate. Use of this homologue resulted in an anaerobic  $\text{H}_2\text{S}$  response up to 750  $\mu\text{M}$ . This sensor could ultimately enable spatially and temporally resolved measurements of  $\text{H}_2\text{S}$  in the gastrointestinal tract to elucidate the role of this metabolite in disease and potentially as a noninvasive diagnostic.

**KEYWORDS:** smart probiotic, diagnostic bacteria, gut inflammation, IBD, sulfur metabolism



## INTRODUCTION

Hydrogen sulfide ( $\text{H}_2\text{S}$ ) is a gaseous metabolite produced by many microbes that inhabit the GI tract.<sup>1</sup> Sulfide has long attracted the attention of researchers due to its unclear, and at times conflicting, role in human GI health and disease.<sup>2,3</sup> Inflammatory bowel disease (IBD) affects 1% of the human population with the incidence rate increasing,<sup>4</sup> partially influenced by the widespread popularization of the Western diet.<sup>5</sup> Beyond genetic predispositions,<sup>6</sup> the onset of IBD is not well characterized mechanistically but it is suspected that microbial dysbiosis may be an agonist.<sup>7</sup> Specifically, metagenomics analysis reveals that sulfate-reducing bacteria (SRB) and enzymes involved in converting cysteine to  $\text{H}_2\text{S}$  are more prevalent in IBD cohorts than in healthy controls.<sup>8</sup> As a molecule genotoxic to enterocytes,  $\text{H}_2\text{S}$  is suggested to have a deleterious role in inflammation through proinflammatory cytokine secretion as a response to DNA damage.<sup>9</sup> Sulfide may also contribute to mucus layer disruption through the reduction of disulfide bonds in the mucin network.<sup>10</sup> However, there is contradictory evidence to support a beneficial role in barrier stability at low levels in ulcerative colitis (UC) mouse models.<sup>11</sup> Overall, the prevailing emerging view is that the effects of sulfide on host health are highly dose-dependent.<sup>12</sup>

Given the dose-dependence of sulfide's physiological effects, accurate measurements of its concentration *in vivo* are crucial.

However, its reactivity and volatility present major technical barriers, resulting in wide estimate ranges for gut  $\text{H}_2\text{S}$  levels (25  $\mu\text{M}$ –2 mM).<sup>13</sup> Additionally, physiological measurements traditionally relied on indirect measurements of stool samples and breath. However, these fail to capture spatial variation in sulfide levels that may occur longitudinally throughout the gut or between the lumen and mucosa. There has been extensive research in electrochemical methods to sense sulfide,<sup>14–16</sup> and a miniaturized capsule system with a wireless transmitter was recently developed,<sup>17</sup> but its use *in vivo* has not been reported.

Diagnostic bacteria engineered with transcriptional biosensors have recently emerged as an attractive route for noninvasive *in vivo* monitoring of a range of gut metabolites.<sup>18</sup> In these systems, a transcription factor responsive to the target ligand is used to control the expression of a reporter protein. Fluorescent reporters provide a convenient readout through the analysis of stool samples by flow cytometry.<sup>19</sup> For more stable readout, sensors can be engineered to regulate DNA

**Received:** February 19, 2025

**Revised:** May 1, 2025

**Accepted:** May 5, 2025

**Published:** May 13, 2025



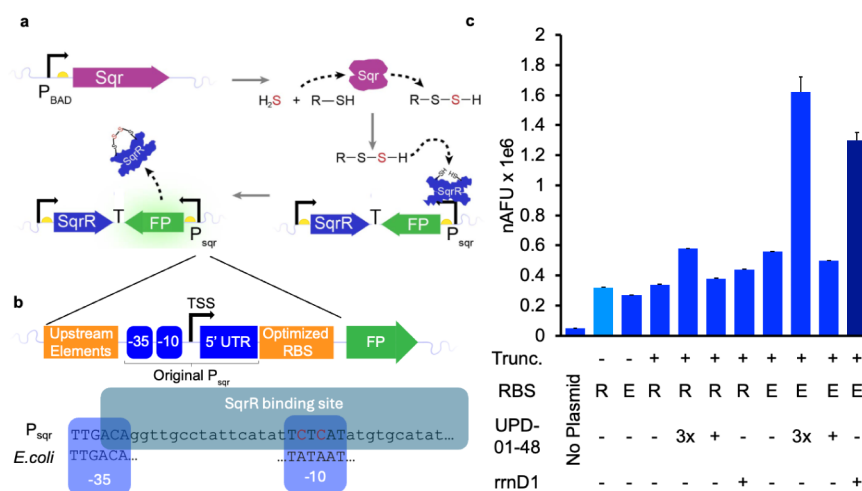


**Figure 1.** Genetic architecture of the  $\text{H}_2\text{S}$  biosensor and engineering to enhance  $P_{\text{sqr}}$  activity. a)  $\text{H}_2\text{S}$  is oxidized to polysulfide by a heterologous sulfide:quinone oxidoreductase (Sqr) expressed from a titratable inducible promoter. Exposed cysteines on the repressor SqrR form a tetrasulfide bridge with the formed polysulfide, resulting in dissociation from the  $P_{\text{sqr}}$  promoter and transcription of the reporter. b) GFP fluorescence from the original and modified  $P_{\text{sqr}}$  promoters in the absence of SqrR, showing combinatorial effects of truncation (Trunc.), new RBS (E for *E. coli* and R for *R. capsulatus*), and inclusion of upstream elements UP-D01-48 or *rrnD1*. A serendipitous cloning error resulted in two additional constructs with 3 tandem UP-D01-48 sequences (3x). The original construct is shown in light blue, and the final optimized in dark blue. c) Detailed view of the  $P_{\text{sqr}}$  showing modifications made to improve activity, including truncation to a core promoter, use of upstream elements, and an optimized ribosome binding site (RBS). nAFU = OD-normalized fluorescence. Bars show mean values of  $n = 3$  biological replicates with error bars showing the standard deviation.

recombinases, encoding the sensing event in the bacteria's DNA.<sup>20</sup> More recently, coupling a luminescence reporter with a miniaturized luminescence detecting and transmitting electronics in an ingestible microbioelectronic device was shown to enable noninvasive real-time readout in pigs.<sup>21</sup> Advances in long-wavelength luminescence reporters also potentially enable the use of biosensors in whole-animal imaging studies to probe specific metabolites with spatial and temporal resolution.<sup>22–25</sup> Finally, transcriptional sensors can be used to actuate a therapeutic response, resulting in a “Smart Probiotic” capable of delivering its payload specifically at sites where the level of the target biomarker indicates disease.<sup>26</sup>

Given the benefits of microbial biosensors and the challenges with traditional measurements of  $\text{H}_2\text{S}$ , we designed and fabricated a transcriptional sulfide biosensor. The ideal sensor would meet the following design parameters: 1) An operational range spanning physiological gut concentrations (25  $\mu\text{M}$ –2 mM); 2) Functionality in both aerobic and anaerobic conditions, owing to the steep radial oxygen gradient from the mucosa to the lumen<sup>27</sup> and the increased concentration of oxygen in sites of inflammation;<sup>28</sup> 3) A highly genetically tractable microbial chassis to allow for rapid sensor characterization and optimization.

## RESULTS AND DISCUSSION

**Sensor Design.** Our strategy was to construct an *E. coli*-based  $\text{H}_2\text{S}$  sensor by adapting the  $\text{H}_2\text{S}$ -responsive regulatory components previously characterized in *Rhodobacter capsulatus*.<sup>29</sup> This microbe uses sulfide as an electron donor for photosynthesis and differentially regulates multiple genes in response to exogenous sulfide. The key regulator is the repressor protein SqrR, which binds the  $\text{sqr}$  promoter ( $P_{\text{sqr}}$ ). In the presence of sulfide, basal expression of sulfide:quinone oxidoreductase (Sqr) catalyzes the oxidation of sulfide to a persulfide. The formed persulfide reacts with two conserved cysteine residues on SqrR to form a tetrasulfide bond that

induces a conformational change, leading to unbinding and derepression of  $P_{\text{sqr}}$ . Our target host was *E. coli*, given the established precedent of using Nissle 1917, a GRAS microbe, in probiotic applications.<sup>30</sup> For development work, here we used *E. coli* S1030, taking advantage of its capacity for titratable arabinose and anhydrotetracycline (aTc) induction.<sup>31</sup> To adapt the sulfide-sensing system to *E. coli*, we used two plasmids with complementary origins of replication (Figure 1a). The first plasmid encodes the sensing module ( $P_{\text{tetR:sqrR}}$ ) and reporting module ( $P_{\text{sqr:gfp}}$ ) in inverse orientation, separated by a bidirectional terminator. The second plasmid contains the oxidation module, with the  $\text{sqr}$  gene under the control of the arabinose promoter ( $P_{\text{bad}}$ ). This design allowed us to separately optimize the  $\text{sqr}$  expression and the persulfide sensing. Initial tests with the system as depicted yielded no detectable response to  $\text{H}_2\text{S}$  (data not shown). We therefore set about optimizing each of the heterologous sensing components for expression in *E. coli*.

**$P_{\text{sqr}}$  Engineering.** We first focused on characterizing and engineering the performance of  $P_{\text{sqr}}$ . Experiments with a control plasmid with GFP under the control of  $P_{\text{sqr}}$  in which the SqrR repressor was removed resulted in minimal GFP expression (Figure 1), suggesting low activity of the native promoter in *E. coli*. One strategy would be to modify the  $-10$  and  $-35$  boxes to be closer to the consensus *E. coli* sequences. However, previous DNA footprinting experiments revealed that the repressor binding site straddled the  $-10$  box<sup>29</sup> (Figure 1c), thus mutating this region would risk losing repressor binding. Instead, we tested combinations of three different alterations: First, the originally cloned  $P_{\text{sqr}}$  sequence included a region of 81 additional base pairs upstream of the  $-35$  box, which we deleted in the case it contained unknown regulatory elements. Second, previous work has identified that upstream elements that precede the  $-35$  box can help recruit Sigma factors to recruit polymerase.<sup>32</sup> We screened two of these, *rrnD1* and UPD-01–48,<sup>33</sup> to assess their impact on GFP

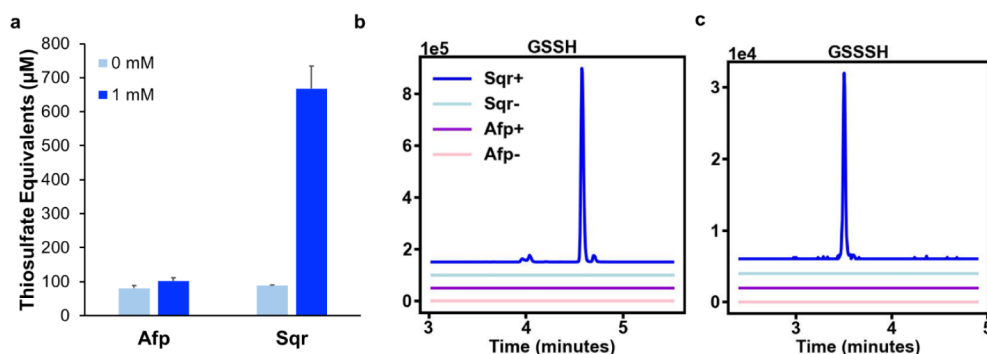


**Figure 2.** Sqr from *Rhodospirillum rubrum* produces glutathione persulfide and glutathione trisulfide from  $\text{Na}_2\text{S}$ . a) Quantification of polysulfides by cyanolysis. Cells harboring  $p_{\text{BAD}}:\text{sqr}$  (Sqr+) or  $p_{\text{BAD}}:\text{mAmetrine}$  (Empty Vector) were grown to  $\text{OD}_{600}$  2.0 and resuspended in HEPES, before being treated with 1 mM  $\text{Na}_2\text{S}$  (bright blue) or vehicle (light blue) and assayed after 1 h. b, c) LC-HRMS of cell lysates from a) after derivatization with monobromobimane. b: Glutathione persulfide (GSSH), XIC of  $m/z$  530.14. c: Glutathione trisulfide (GSSSH), XIC of  $m/z$  562.09. Data shown are averages of  $n = 3$  biological replicates with error bars showing one standard deviation.

expression. Lastly, using the ribosome binding site (RBS) calculator,<sup>34</sup> we designed a new sequence to replace the native *R. capsulatus* to improve translation rates. Each of these modifications was screened individually, and in combination. The resultant impact on GFP expression is shown in Figure 1c.

Individually, these changes had minor effects on GFP expression. However, the combination of truncation, a new RBS, and UP-D01-48 resulted in a 1.5-fold increase in fluorescence compared to that of the original construct. Changing the upstream element to *rrnD1* with the other two changes outperformed UP-D01-48, yielding a 4.5-fold increase in fluorescence compared with the original promoter. Interestingly, a version of the construct with three tandem repeats of UP-D01-48 derived from a serendipitous assembly product during cloning resulted in a 5.5-fold increase in fluorescence. Given that repeat sequences can be unstable<sup>35</sup> and that fluorescence from this construct was only marginally brighter than the *rrnD1* version, we selected the latter for sensor development.

**Sqr Characterization.** With the reporting module in hand, we next confirmed the functionality of Sqr, which catalyzes the oxidation of sulfide into polysulfides for binding with SqrR. Sqr activity in whole cells was quantified using cyanolysis.<sup>36</sup> As shown in Figure 2a, the enzyme was highly active, converting 70% of sulfide to polysulfide within 1 h. We then sought to identify the specific products of the reaction, as Sqr can use a variety of compounds as the sulfane sulfur acceptor, including sulfide, sulfite, and low-molecular-weight thiols like glutathione (GSH).<sup>37</sup> Given the high concentration of GSH in *E. coli*,<sup>38</sup> we suspected that GSH was the predominant cosubstrate. Cell lysates were derivatized with monobromobimane and analyzed by LC-HRMS, revealing glutathione per- and trisulfide as the only products with an increased peak area compared to empty-vector and no-sulfide controls (Figure 2b,c and Table S1).

**SqrR Soluble Expression.** We next optimized the sensing module. The initial sensor designed used  $P_{\text{Tet}}$  for the inducible expression of SqrR to allow titration of the repressor. Unfortunately, GFP expression from the  $P_{\text{Tet}}:\text{SqrR } P_{\text{Sqr}}:\text{GFP}$  expression at full induction was no different than that of control constructs without SqrR, suggesting low expression of the repressor. We replaced  $P_{\text{Tet}}$  with  $P_{\text{J23100}}$ , a strong constitutive promoter, but this still resulted in no repression of  $P_{\text{Sqr}}$  promoter activity (Figure 3), suggesting the problem might not be the level of expression, but the solubility of SqrR. In previous work, SqrR was purified with an N-terminal His<sub>6</sub>-

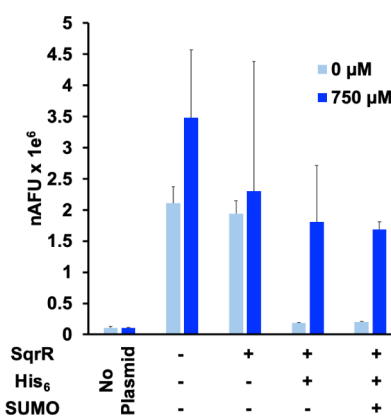


**Figure 3.** Enhancing SqrR solubility with N-terminal tags results in sulfide-dependent regulation of  $P_{\text{Sqr}}$ . Bars represent mean OD-normalized fluorescence 16 h after addition of 750  $\mu\text{M}$  sulfide (bright blue) or vehicle (light blue) in  $n = 3$  biological replicates. Error bars represent one standard deviation.

SUMO tag to assist in protein folding.<sup>29</sup> We therefore explored constructs containing either His<sub>6</sub>-SUMO, or a His<sub>6</sub> tag alone, which has also been shown to improve soluble expression.<sup>39</sup> Both tag configurations resulted in soluble expression, as indicated by the complete repression of GFP expression in the absence of sulfide (Figure 3). Excitingly, the addition of 750  $\mu\text{M}$   $\text{Na}_2\text{S}$  in cells expressing Sqr resulted in a 9.8 and 8.2-fold derepression for the His<sub>6</sub> tag and His<sub>6</sub>-SUMO tag, respectively, compared with their untreated controls. Since the derepressed expression level was more consistent with the His<sub>6</sub>-SUMO tag ( $p = 0.00058$  vs  $p = 0.026$ ), we selected this one for the final sensor design.

**Aerobic Sensor Performance.** With the individual components optimized, we next characterized the full sensor's performance. While microtiter plate-based assays are convenient for biosensor optimization, initial experiments in 96-well plates resulted in no GFP fluorescence (data not shown), likely due to the volatility of sulfide under the slightly acidic culture conditions ( $\text{pK}_a = 7.0$ ). By contrast, cultures sealed in Hungate tubes with a headspace of air demonstrated a modest sulfide-dependent response up to 250  $\mu\text{M}$  sulfide (Figure S2). Sqr couples sulfide oxidation to the reduction of a quinone, and sustained activity relies on the reoxidation of the quinol by oxygen through the electron transport chain. We hypothesized that oxygen availability in the Hungate tubes may limit the

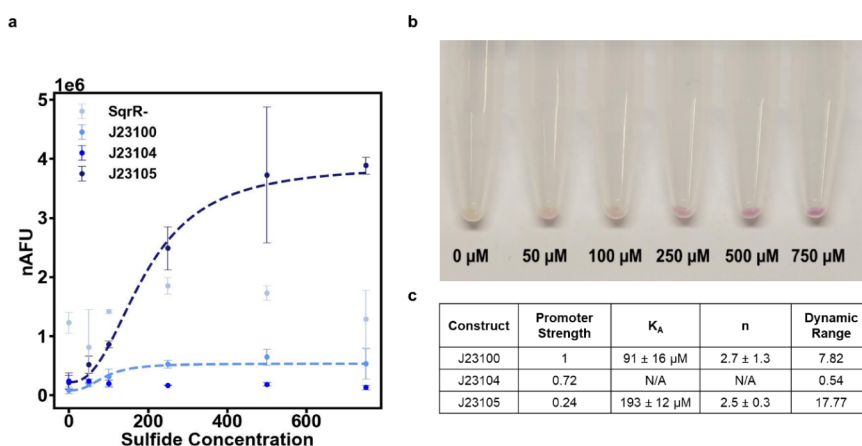


**Figure 4.** SqrR titration improves sensor performance. (a) OD-normalized fluorescence 16 h after sulfide addition for various sensor constructs as a function of concentration. For J23100 and J23105, Hill parameters were fitted to the experimental data, and curves are shown as dotted lines. Data points are means of  $n = 3$  biological replicates. Error bars are  $\pm$  one standard deviation. (b) Pellets from the J23105-based sensor with sulfide exposure increasing left to right show visible increase in red color from mKate. (c) Table of parameters for the 3 sensor constructs, showing half-maximal ligand occupation ( $K_A$ ), cooperativity ( $n$ ) and dynamic range. Hill parameters are presented with 95% confidence intervals.

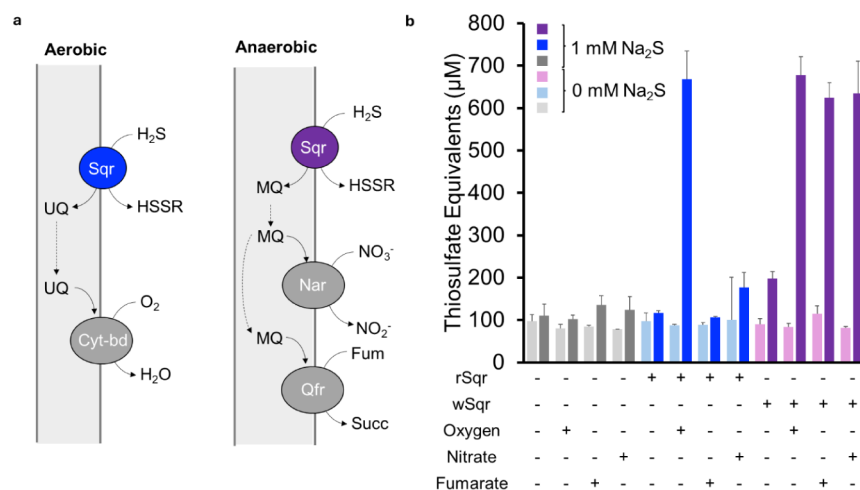


**Figure 5.** Sqr from *Wolinella succinogenes* enables anaerobic conversion of sulfide to polysulfides. a) Schematic of electron transfer from sulfide to terminal different electron acceptors until aerobic (left) or anaerobic (right) conditions. b) Quantification of Sqr activity by cyanolysis with the *Wolinella* (wSqr) and *Rhodobacter* (rSqr) homologues under aerobic conditions and in anoxic environments with or without 20 mM sodium nitrate or sodium fumarate. Bars represent means of  $n = 3$  biological replicates, with error bars representing one standard deviation. Abbreviations: UQ, ubiquinone; MQ, menaquinone; HSSR, polysulfide; Cyt-bd, cytochrome oxidase; Nar, nitrate reductase; Qfr, quinone:fumarate reductase.

oxidation of higher concentrations of sulfide, reducing the operational range. To test this, we increased the surface area and headspace-to-volume ratio of the cultures by switching from Hungate tubes (5 mL culture per 17 mL tube) to serum bottles (10 mL culture per 120 mL bottle). Excitingly, this increased the upper limit of the operational range from 250 to 750  $\mu\text{M}$  (Figure S2), at a slight cost of dynamic range (6.2 vs 4.7).

With a working sensor in hand, we investigated additional opportunities to expand the dynamic range. By switching the reporter to mKate, the dynamic range increased by 35% (Figure S3), presumably because of decreased background autofluorescence, so we used mKate for all subsequent work. At this point, the sensor only recovered 40% of the hypothetical dynamic range compared to a SqrR-negative control. We hypothesized that the strong promoter (J23100) driving *sqrR* was producing repressor in excess of the intracellular persulfide concentration, even at high levels of  $\text{H}_2\text{S}$ . To test this, we titrated *sqrR* expression, reducing the

promoter strength by approximately 28% and 76% with J23104 and J23105, respectively. Excitingly, the dynamic range increased from 8 to 18 with the J23105 promoter (Figure 4a). Most intriguingly, the fluorescence values of the J23105-based sensor above 250  $\mu\text{M}$  sulfide were higher than those in the unrepressed control lacking *sqrR* (Figure 4a). Both the original J23100-based sensor and the J23105 variant exhibited a sigmoidal dependence on sulfide, with a  $K_A$  of  $91 \pm 16 \mu\text{M}$  and  $n$  of  $2.7 \pm 1.3$  for J23100, and a  $K_A$  of  $193 \pm 12 \mu\text{M}$  and  $n$  of  $2.5 \pm 0.3$  for J23105.

**Engineering the Sensor to Work Anaerobically.** As described above, sustained Sqr activity depends on the continuous reoxidation of the quinol pool through the electron transport chain. In the previous experiments, oxygen served as the terminal electron acceptor, but the gut microbiota is primarily anaerobic. Fumarate and nitrate are two alternative electron acceptors found in the GI tract, with fumarate abundant in the healthy gut,<sup>40</sup> and elevated nitrate associated with inflammation.<sup>41</sup> Both are reduced in *E. coli* by quinol-

dependent reductases. We thus hypothesized that the sulfide sensor should function anaerobically in the presence of these compounds. Unfortunately, in contrast to previous observations,<sup>42</sup> in our hands the *Rhodobacter* Sqr showed minimal activity anaerobically with either of these electron acceptors by cyanolysis assay (Figure 5a).

We suspected that this may be due to a mismatch between the quinone specificity of Sqr and the quinones available during aerobic and anaerobic growth (Figure 5b). Under aerobic conditions, ubiquinone is the dominant quinone in *E. coli*,<sup>43</sup> but under anaerobic conditions menaquinone becomes the primary.<sup>44</sup> We hypothesized that the *Rhodobacter* Sqr may have minimal activity with menaquinone, preventing robust anaerobic activity, consistent with the role of this enzyme in aerobic sulfide oxidation.<sup>45</sup> To overcome this challenge, we sought to identify an alternative Sqr that used menaquinone as a redox cofactor. Given that every characterized fumarate reductase is menaquinone-dependent,<sup>46</sup> we reasoned that an Sqr from an organism that could couple sulfide oxidation to nitrate reduction would likely be menaquinone-specific. *Wolinella succinogenes* is an obligate anaerobe that was shown to couple sulfide oxidation to fumarate reduction for growth,<sup>47</sup> though an Sqr was neither identified nor characterized. Using the *Rhodobacter* Sqr (rSqr) sequence as a BLAST query, we identified an Sqr homologue in *W. succinogenes* (Accession # WP\_011138184.1). The corresponding gene was amplified from *Wolinella* gDNA and the putative Sqr was tested under both aerobic and anaerobic conditions, with fumarate and nitrate available as anaerobic electron acceptors. Remarkably, *Wolinella* Sqr (wSqr) could perform sulfide oxidation with a similar yield under both aerobic and anaerobic conditions (Figure 5b).

The capability of *Wolinella* Sqr (wSqr) to oxidize sulfide in *E. coli* under anaerobic conditions was promising for developing an anaerobic biosensor. We next incorporated this gene into the oxidation module of the sensing strains, and tested the sensor anaerobically, using aerobic fluorescence recovery to detect mKate fluorescence.<sup>48</sup> As shown in Figure 6, the anaerobic sensor with the wSqr responded over a similar range of sulfide concentrations with slightly different dynamics. With fumarate in the culture media, the sensor produced a binary response: While there was no increase in fluorescence between 50 and 250  $\mu\text{M}$  (Figure S4), there was a significant increase at concentrations above 500  $\mu\text{M}$  ( $p = 0.0099$ ), with a similar dynamic range as the aerobic sensor (15.7 vs 18, respectively). With nitrate, there was a 5.7-fold response at 750  $\mu\text{M}$ , but it was not statistically significant ( $p = 0.068$ ), and there appeared to be a more graded but statistically insignificant concentration-dependent response (Figure S4).

The dynamic range of the sensor with fumarate was similar to the output with rSqr under aerobic conditions. Interestingly, as with the aerobic sensor, the fully induced expression is higher than that of the no-SqrR control. The reason for the limited resolution of intermediate sulfide concentrations is presently unclear. However, the sensor can clearly delineate between physiologically low and high levels, which could eventually be useful in a clinical or diagnostic context, especially given the challenges with current methodologies for  $\text{H}_2\text{S}$  detection.

Finally, as a first step toward translating the sensor to the more complex gut environment, we examined the specificity of the sensor for sulfide, testing whether other sulfur compounds in the gastrointestinal tract cross-reacted. Specifically, we tested

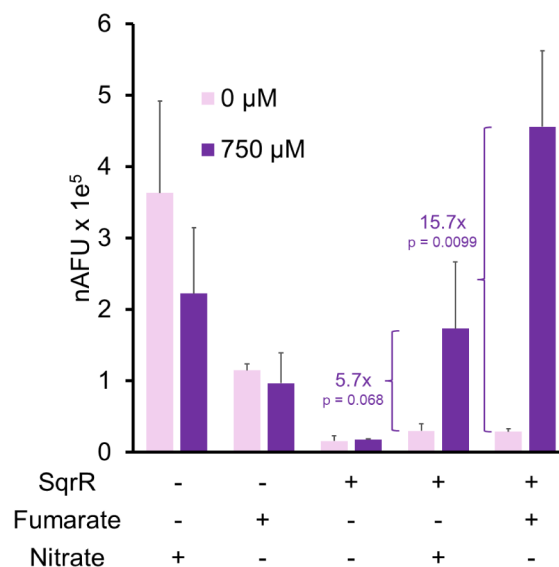


**Figure 6.** Anaerobic sensor discriminates between physiologically high and low levels of sulfide. Normalized fluorescence values of the wSqr-based sensor under anaerobic conditions with either fumarate or nitrate and with or without 750  $\mu\text{M}$  sodium sulfide. Bars represent means of  $n = 3$  biological replicates with error bars of one standard deviation.  $p$ -values are from one-sided paired  $t$  tests comparing normalized fluorescence between treatments.

sulfate, sulfite, thiosulfate, and a polysulfide mix (Figures S2–S5, Tables S6 and S7, and Note S8), using sensor strains with or without expression of wSqr. As expected, given that SqrR responds to polysulfides, in the absence of Sqr, only cells treated with polysulfide showed significantly increased fluorescence (Figure S5a). The response was much weaker (1.45-fold induction) than that with an equal concentration of sulfide using the full sensor, which we speculate is due to either poor transport of polysulfides across the cell membrane or their spontaneous degradation under aqueous conditions.

In the full sensor with Sqr present, neither sulfate nor thiosulfate elicited a response. This is encouraging because these are major sulfur sources in the gut.<sup>19</sup> Polysulfide exhibited a much higher response (3.6-fold induction) with Sqr present than without. We hypothesize this is due to the oxidation of sulfide released from the abiotic breakdown of polysulfides, which are known to be highly unstable and easily hydrolyzed.<sup>49</sup> Consistent with this, sulfide was detected in the medium of cells treated with polysulfide (Figure S5b). Most interestingly, in the Sqr background, sulfite also resulted in a significant fluorescent signal (3.6-fold induction). We initially hypothesized that sulfite was reduced to sulfide by the *E. coli* sulfite reductase, and then oxidized by Sqr to form polysulfides that interact with SqrR. However, in a follow-on experiment in which cells without Sqr were treated with sulfite, no sulfide was detected in the media (Figure S5b). How sulfite results in the derepression of SqrR only in an Sqr background is presently unclear, but it is worth noting that sulfite has been shown in the absence of sulfide to form a kinetically competent complex with human SQR.<sup>50</sup> Overall, these results suggest that the only cross-talk we expect in the gut is with polysulfide and sulfite. Polysulfides are highly unstable, and when measured in feces have been found to be  $\sim 50$ -fold lower in concentration than sulfide,<sup>51</sup> suggesting they are unlikely to cause interference. The level of sulfite in the gut is unclear.

To the best of our knowledge, this work is the first report of a transcriptional biosensor for the detection of exogenous sulfide under both aerobic and anaerobic conditions. A previous report<sup>52</sup> detailed the construction of a similar reporter consisting of the persulfide-responsive CstR repressor and cognate promoter from *Staphylococcus aureus*, and Sqr from *Cupriavidus pinatubonensis* or *Pseudomonas putida*. However, fluorescence output from the reporter strain saturated at 10  $\mu\text{M}$   $\text{H}_2\text{S}$ , which is in the range produced by WT *E. coli*. Thus, the authors focused instead on using their sensor as an elegant quorum-sensing system. As shown in Figures 5 and 6, our sensor is responsive to much higher concentrations of sulfide, allowing it to reliably detect different levels of exogenously supplied sulfide within the physiologically relevant range found within the gut.<sup>13</sup> We speculate that the key difference is the relative sensitivity of CstR and SqrR to persulfide, given that these proteins are from different families.<sup>29</sup>

Given its ability to detect elevated levels of sulfide both aerobically and anaerobically, and the high specificity for sulfide, the sensor developed here may have promise as a noninvasive diagnostic tool. Additionally, our demonstration of a strain capable of anaerobically oxidizing sulfide could eventually lead to new therapeutics based on engineered probiotics, given that compromised sulfide oxidation capacity is associated with IBD.<sup>53</sup> The sensor could also find use in other anoxic environments where sulfide plays an important physiological role, such as the tumor microenvironment.<sup>54</sup> In the future, the sensor could be engineered into probiotic strains designed to modulate  $\text{H}_2\text{S}$  levels *in vivo*.<sup>55</sup>

There are several remaining challenges that must be overcome for the implementation of the sensor in the gut microenvironment. *E. coli* S1030 was used in this work because of the convenience of its titratable arabinose and aTc induction. However, it is not a GRAS strain,<sup>30</sup> and some additional reoptimization may be necessary when transferring the sensor components into a more appropriate host for *in vivo* work like *E. coli* Nissle 1917. Sensor performance must also be verified over the physiological pH range found in the gut (5.5–7.4).<sup>56</sup> Additionally, the concentrations of fumarate and nitrate tested here (20 mM) are likely much higher than those available in the gut, and how the levels of these electron acceptors impact sensor performance remains to be determined. Finally, we have shown the sensor to be relatively specific for sulfide, with no response to abundant sulfur sources such as sulfate and thiosulfate. However, sulfite and polysulfide do activate the sensor. How sulfite activates the sensor in an Sqr-dependent manner is unclear and provides fertile ground for future biochemical work, but one potential solution to eliminate crosstalk from both compounds may be to identify and delete transporters responsible for their uptake into *E. coli*. Despite these challenges, taken together this work provides the foundational genetic elements required for selective sulfide sensing in the anaerobic gut microenvironment.

Beyond the practical utility of the sensor, an additional interesting finding from this work was the importance of the HIS<sub>6</sub>-SUMO tag to the functionality of the repressor. Metagenomic screening has emerged as a promising method of identifying new transcription factors responsive to a wide range of chemical ligands.<sup>57</sup> Such screens should consider the use of such tags to enhance the solubility of heterologous regulators and avoid false negatives. The use of UP elements to enhance transcription from a suboptimal promoter may also prove to be a general strategy for engineering novel

transcriptional machinery into heterologous hosts. Overall, this work provides a sensitive transcriptional sulfide biosensor that could be used in diagnostic situations as well as novel approaches to the optimization of biosensors based on heterologous transcription factors.

## MATERIALS AND METHODS

**Media and Chemicals.** All chemicals were purchased from Fisher Scientific unless otherwise stated. Bacterial strains were cultured in either Luria–Bertani (LB) medium containing 5 g/L yeast extract, 10 g/L tryptone, and 10 g/L NaCl or a supplemented M9 medium (M9+). M9+ contained 6 g/L  $\text{Na}_2\text{HPO}_4$ , 0.5 g/L NaCl, 3 g/L  $\text{KH}_2\text{PO}_4$ , 1 g/L  $\text{NH}_4\text{Cl}$ , 1 mM  $\text{MgSO}_4$ , 0.1 mM  $\text{CaCl}_2$ , 4 g/L glucose, 1 g/L Casamino acids, and 1 mg/L thiamine-HCl. Carbenicillin (100  $\mu\text{g/L}$ ) and spectinomycin (60  $\mu\text{g/L}$ ) were used for plasmid maintenance, and chloramphenicol was used for growth inhibition during aerobic fluorescence recovery experiments at 20  $\mu\text{g/L}$ . Induction of *sqr* was achieved through the addition of 10 mM L-arabinose.

**Plasmid Construction and Strains.** Bacterial strains used in this work are listed in Table S6. *E. coli* s1030 was chosen as the final sensor strain, as it carries a genomic copy of *tetR* to enable anhydrotetracycline (aTc) induction and constitutive *araE* expression for titratable arabinose induction.<sup>31</sup> All cloning was performed in *E. coli* DH5a (New England Biolabs, NEB). Medium copy-number plasmids pTR47 (SpR) and pTR48 (AmpR)<sup>58,59</sup> were chosen for the sensor cassette and Sqr expression, respectively. PCR and Gibson assembly were performed using Q5 Polymerase and Hi-Fi Assembly Mix (NEB). Constructs were verified by sequencing (Azenta/Primordium). DNA and plasmid purification kits were purchased from Zymo Research. *Rhodobacter capsulatus* genes were codon harmonized<sup>60</sup> and synthesized as gBlocks by Integrated DNA Technologies. Promoter configurations were sampled through overlap extension PCR from the Andersen library series (iGEM Part:BBa\_J23100) for *sqrR* expression. HIS<sub>6</sub>-SUMO tag, GFP, mKate, and pBAD elements were PCR-amplified from the plasmids shown in Table S1. *Wolinella succinogenes* was purchased from DSMZ and the *sqr* gene was amplified from genomic DNA. Final plasmids were transformed into chemically competent *E. coli* s1030 using heat shock.<sup>61</sup> Single colony isolates were selected off antibiotic agar plates and grown in LB overnight before cryopreserved in 20% glycerol at  $-80$  °C. All plasmids and primer sequences can be found in Tables S6 and S7 respectively. DNA sequences of relevant components are listed in Note S8. Plasmid maps are given in Figure S9. The final biosensor constructs are available from AddGene.

**Sensor Assay. Aerobic Sensor Experiments.** Overnight cultures were diluted 1:100 in fresh M9+ medium in shake flasks at 200 rpm with carbenicillin, spectinomycin, and L-arabinose. Cells were grown at 37 °C until OD 0.3, then 10 mL were aliquoted into 120 mL serum bottles. Sodium sulfide ( $\text{Na}_2\text{S}$ )—prepared as a stock solution at 100 mM in 100 mM NaOH—was added to the desired concentration, and cultures were quickly sealed with butyl rubber septa and aluminum crimp seals to minimize  $\text{H}_2\text{S}$  evaporation. Sulfide assays were conducted at this point to confirm the initial concentration. Vessels were then returned to the shaker for 12–18 h, after which 200  $\mu\text{L}$  samples were transferred to a 96-well plate for measurements of OD<sub>600</sub> and fluorescence (SpectraMax i3, Molecular Devices). GFP and mKate measurements were

taken at wavelength pairings 485/515 and 585/635 respectively. When used in sensor experiments, stocks of sodium sulfate, sodium thiosulfate, sodium sulfite, and potassium polysulfide (Figures S2–S5, Tables S6 and S7, Note S8) were prepared fresh in DI water at a concentration of 100 mM to ensure the total volume of liquid added was the same as for the sulfide control.

**Anaerobic Sensor Experiments.** For anaerobic experiments, precultures were grown anaerobically from cryostocks in M9+ medium in Hungate tubes overnight. Following the same dilution as above, serum bottles were prepared in the anaerobic chamber using degassed medium and electron acceptors (20 mM sodium nitrate or 20 mM sodium fumarate) and transferred to the shaker. After the cells reached an OD<sub>600</sub> of 0.3, they were returned to the chamber and split into 6 individual serum bottles (10 mL) for each sulfide level following the same timeline as stated above and received sulfide from stock solution prepared anaerobically. For fluorescent sampling, GFP matured in minutes following withdrawal by syringe and needle, and was measured immediately. Samples taken from mKate matured more slowly and were treated with chloramphenicol to inhibit protein synthesis during a 2 h aerobic maturation prior to recording the final fluorescence value.

All sensor outputs are reported as normalized Arbitrary Fluorescence Units (nAFU), which are media-blank-adjusted fluorescence outputs divided by media-blank-adjusted OD<sub>600</sub>:

$$\text{nAFU} = \frac{\text{AFU} - \text{AFU}_{\text{blank}}}{\text{OD}_{600} - \text{OD}_{600,\text{blank}}} \quad (1)$$

Where appropriate, sensor data were fitted to the Hill equation (eq 2) using SciPy's `curve_fit` in Python for plotting and parameter estimation:

$$\text{nAFU} = \frac{[\text{S}^{2-}]^n}{K_A^n + [\text{S}^{2-}]^n} \cdot \text{nAFU}_{\text{max}} + \text{nAFU}_{\text{min}} \quad (2)$$

where nAFU<sub>max</sub> is the fluorescence at the highest level of sulfide and nAFU<sub>min</sub> is fluorescence with no sulfide.

**Statistics.** Where indicated in the text, *p*-values are calculated by performing a paired, one-tailed *t*-test of nAFU calculated between the designated sulfide level and untreated control.

**Methylene Blue Sulfide Assay.** To confirm sulfide concentrations in liquid samples, we used the previously adapted methylene blue assay modified for a 96-well plate format.<sup>55</sup> Briefly, 200 μL of cell culture sample was added to a mixture containing 600 μL of 1% (w/v) zinc acetate and 15 μL of 3 N NaOH, and the mixture was vortexed. Following a 5 min incubation period, 150 μL of 0.1% *n*-dimethylethylenediamine in 5 N HCl and 150 μL of 23 mM ferric chloride in 1 N HCl were added. Samples were then centrifuged at 16,000 *g* for 5 min. 200 μL of the supernatant was transferred to a 96-well plate for absorbance measurement at 670 nm and compared to a standard curve prepared in the identical medium.

**Hot Cyanolysis for Polysulfide Quantification.** To quantify Sqr activity, a cyanolysis procedure was adapted from ref. 36. Overnight cultures were diluted 1:100 in LB and grown to OD 0.3 before adding 10 mM L-arabinose and cultured for an additional 3 h. Cells were harvested by centrifugation at 3,000 *g* for 10 min and washed in 1/10 culture volume of 50 mM HEPES (pH 7.0) before resuspension to OD<sub>600</sub> of 2.0 in the same buffer. 3 mL of cell suspension was then aliquoted

into Hungate tubes, treated with 1 mM Na<sub>2</sub>S and shaken at 37 °C for 1 h before sample collection. 250 μL of cell suspension was added to preprepared microcentrifuge tubes containing 550 μL of 1% boric acid (w/v in water) and 200 μL of 100 mM potassium cyanide. Samples were then boiled using a heat block at 100 °C for 5 min, and cooled to room temperature. Then, 100 μL of ferric nitrate reagent (3 g of ferric nitrate in 5 mL of 33% perchloric acid) was added to each sample and centrifuged at 16,000 *g* for 5 min. 200 μL of supernatants of samples was transferred to a 96-well plate and absorbance was recorded at 460 nm. Quantification was achieved through comparison to a standard curve of sodium thiosulfate, processed in the same way but with the addition of 5 μL of 1 M copper sulfate as a catalyst for thiosulfate conversion.

**Identification of Sqr Products by LC-HRMS.** 1.5 mL of cells from the cyanolysis experiments described above was centrifuged and the resulting pellets were frozen at –80 °C for analysis of reaction products by LC-HRMS following derivatization with monobromobimane (mBBr).<sup>62</sup> Lysis and derivatization were accomplished in a single step using a lysis buffer consisting of 50% v/v acetonitrile in water with 20 mM ammonium bicarbonate and 5 mM mBBr, prepared fresh daily and covered in foil to prevent light exposure. Cell pellets were resuspended in 200 μL of mBBr lysis buffer and mixed by pipetting. Samples were incubated at 60 °C for 1 h in the dark with a heat block covered in foil. Samples were then centrifuged at 20,000 *g* for 10 min to precipitate cellular debris. Supernatants were diluted 5-fold in LCMS-grade water and then filtered via syringe (0.2 μm filter) into vials. Samples were analyzed on an Agilent 6545 LC-MS QTOF equipped with an electrospray ionization (ESI) source and an Agilent Zorbax Eclipse Plus C18 UPLC column. Mobile phase A was 0.1% formic acid in water, mobile phase B was 95% acetonitrile with 5% water, and all solvents were LCMS grade. The gradient started at 98% mobile phase A, and ramped to 2% mobile phase B over 7.5 min, at 0.4 mL/min with a column temperature of 40 °C. The QTOF was operated in positive mode, using a fragmentor voltage of 125 V. The MS scan range was 100 to 1700 *m/z*, with a resolution of approximately 20,000 for 500 *m/z*. Predicted compound formulas of polysulfide products were used with the Find By Formula tool in Agilent's MassHunter software to identify polysulfide peaks. Find By Formula identified the peaks using the exact mass, natural isotope spacing, and abundance predicted from the compound formula. Retention times were obtained from derivatized standards where possible.

## ■ ASSOCIATED CONTENT

### SI Supporting Information

The Supporting Information is available free of charge at <https://pubs.acs.org/doi/10.1021/acssynbio.5c00124>.

The supplementary document includes a full description of sulfur compounds identified by LC-HRMS, additional data supporting the choice of culture conditions and fluorescent proteins, complete performance data for the anaerobic sensor construct, and analysis of the specificity of the sensor. It also includes tables of the strains, plasmids and oligos used in this work, along with sequences of key genes and regulatory elements and plasmid maps (PDF)

## AUTHOR INFORMATION

### Corresponding Author

Benjamin M. Woolston – Department of Chemical Engineering, Northeastern University, Boston, Massachusetts 02115, United States; Department of Bioengineering, Northeastern University, Boston, Massachusetts 02115, United States; [orcid.org/0000-0002-6570-2236](https://orcid.org/0000-0002-6570-2236); Email: [b.woolston@northeastern.edu](mailto:b.woolston@northeastern.edu)

### Authors

Matthew T. Fernez – Department of Chemical Engineering, Northeastern University, Boston, Massachusetts 02115, United States

Shanthi Hegde – Department of Biology, Northeastern University, Boston, Massachusetts 02115, United States

Justin A. Hayes – Department of Chemical Engineering, Northeastern University, Boston, Massachusetts 02115, United States

Kathryn O. Hoyt – Department of Chemical Engineering, Northeastern University, Boston, Massachusetts 02115, United States

Rebecca L. Carrier – Department of Chemical Engineering, Northeastern University, Boston, Massachusetts 02115, United States; Department of Bioengineering, Northeastern University, Boston, Massachusetts 02115, United States; [orcid.org/0000-0003-3002-7098](https://orcid.org/0000-0003-3002-7098)

Complete contact information is available at:

<https://pubs.acs.org/10.1021/acssynbio.5c00124>

### Author Contributions

M.T.F., B.M.W., and R.L.C. conceived this project. M.T.F. and B.M.W. designed the constructs and experiments. M.T.F. carried out the experiments and analyzed the data. S.H. helped with cloning and testing of *Wolinella* Sqr constructs. J.A.H. optimized and assisted in chemical sulfide measurements. M.T.F. and B.M.W. prepared and revised the manuscript. All authors approved the final version of the manuscript.

### Notes

The authors declare the following competing financial interest(s): J.A.H. is the co-founder and affiliated with Concordance Therapeutics Inc, a company developing engineered probiotics for modulation of sulfur metabolism for therapeutic applications.

## ACKNOWLEDGMENTS

The authors thank David Liu's lab for the donation of pTR47 and pTR48. This work was also advanced by the contributions from undergraduates Brielle Quigley, Ella Sweet, and Julia Chen, who assisted in sensor experiment execution. The authors are grateful for financial support to BMW from an NIH NBIB Trailblazer (R21EB033892) and to RLC from an NIH NIBIB R01 (1R01EB021908). Figures were prepared with BioRender.

## ABBREVIATIONS

IBD	inflammatory bowel disease
GI	gastrointestinal
H <sub>2</sub> S	hydrogen sulfide
Sqr	sulfide:quinone (oxido)reductase
SRB	sulfate-reducing bacteria
UC	ulcerative colitis
nAFU	normalized arbitrary fluorescence units

LC-HRMS	liquid chromatography-high-resolution mass spectrometry
mBBr	monobromobimane
TSS	transcription start site
RBS	ribosome binding site.

## REFERENCES

- (1) Carbonero, F.; Benefiel, A. C.; Alizadeh-Ghamsari, A. H.; Gaskins, H. R. Microbial pathways in colonic sulfur metabolism and links with health and disease. *Front. Physiol.* **2012**, *3*, 00448.
- (2) Singh, S. B.; Lin, H. C. Hydrogen Sulfide in Physiology and Diseases of the Digestive Tract. *Microorganisms* **2015**, *3*, 866–889.
- (3) Buret, A. G.; Allain, T.; Motta, J. P.; Wallace, J. L. Effects of Hydrogen Sulfide on the Microbiome: From Toxicity to Therapy. *Antioxid. Redox Signal.* **2022**, *36*, 211–219.
- (4) Guan, Q. A Comprehensive Review and Update on the Pathogenesis of Inflammatory Bowel Disease. *J. Immunol. Res.* **2019**, *2019*, 7247238.
- (5) Chiba, M.; Nakane, K.; Komatsu, M. Westernized Diet is the Most Ubiquitous Environmental Factor in Inflammatory Bowel Disease. *Perm J.* **2019**, *23* (1), 18–107.
- (6) Strober, W.; Kitani, A.; Fuss, I.; Asano, N.; Watanabe, T. The molecular basis of NOD2 susceptibility mutations in crohn's disease. *Mucosal Immunol.* **2008**, *1*, S5–S9.
- (7) Santana, P. T.; et al. Dysbiosis in Inflammatory Bowel Disease: pathogenic Role and Potential Therapeutic Targets. *Int. J. Mol. Sci.* **2022**, *23* (7), 3464.
- (8) Kushkevych, I.; Sangrador, J. C.; Dordević, D.; Rozehnalová, M.; Černý, M.; Fafula, R.; Vítězová, M.; Rittmann, S. K.-M. R.; et al. Evaluation of physiological parameters of intestinal sulfate-reducing bacteria isolated from patients suffering from ibd and healthy people. *J. Clin. Med.* **2020**, *9* (6), 1920.
- (9) Mottawea, W.; et al. Altered intestinal microbiota-host mitochondria crosstalk in new onset Crohn's disease. *Nat. Commun.* **2016**, *7*, 13419.
- (10) Ijssennagger, N.; et al. Gut microbiota facilitates dietary heme-induced epithelial hyperproliferation by opening the mucus barrier in colon. *Proc. Natl. Acad. Sci. U. S. A.* **2015**, *112*, 10038–10043.
- (11) Motta, J. P.; et al. Hydrogen sulfide protects from colitis and restores intestinal microbiota biofilm and mucus production. *Inflamm. Bowel Dis.* **2015**, *21*, 1006–1017.
- (12) Xu, W.; Watanabe, K.; Mizukami, Y.; Yamamoto, Y.; Suzuki, T. Hydrogen sulfide suppresses the proliferation of intestinal epithelial cells through cell cycle arrest. *Arch. Biochem. Biophys.* **2021**, *712*, 109044.
- (13) Buret, A. G.; Allain, T.; Motta, J. P.; Wallace, J. L. Effects of Hydrogen Sulfide on the Microbiome: From Toxicity to Therapy. *Antioxid. Redox Signal.* **2022**, *36*, 211.
- (14) Xu, T.; et al. Electrochemical hydrogen sulfide biosensors. *Analyst* **2016**, *141*, 1185–1195.
- (15) Shah, S. S.; Aziz, M. A.; Oyama, M.; Al-Betar, A. R. F. Controlled-Potential-Based Electrochemical Sulfide Sensors: A Review. *Chem. Rec.* **2021**, *21*, 204–238.
- (16) Brown, M. D.; Hall, J. R.; Schoenfish, M. H. A direct and selective electrochemical hydrogen sulfide sensor. *Anal. Chim. Acta* **2019**, *1045*, 67–76.
- (17) Stine, J. M.; Ruland, K. L.; Beardslee, L. A.; Levy, J. A.; Abianeh, H.; Botasini, S.; Pasricha, P. J.; Ghodssi, R.; et al. Miniaturized Capsule System Toward Real-Time Electrochemical Detection of H<sub>2</sub>S in the Gastrointestinal Tract. *Adv. Healthcare Mater.* **2024**, *13* (5), 2302897.
- (18) Tanna, T.; Ramachandran, R.; Platt, R. J. Engineered bacteria to report gut function: technologies and implementation. *Curr. Opin. Microbiol.* **2021**, *59*, 24–33.
- (19) Daeffler, K. N.; Galley, J. D.; Sheth, R. U.; Ortiz-Velez, L. C.; Bibb, C. O.; Shroyer, N. F.; Britton, R. A.; Tabor, J. J.; et al. Engineering bacterial thiosulfate and tetrathionate sensors for detecting gut inflammation. *Mol. Syst. Biol.* **2017**, *13* (4), 923.

- (20) Naydich, A. D.; Nangle, S. N.; Bues, J. J.; Trivedi, D.; Nissar, N.; Inniss, M. C.; Niederhuber, M. J.; Way, J. C.; Silver, P. A.; Riglar, D. T.; et al. Synthetic Gene Circuits Enable Systems-Level Biosensor Trigger Discovery at the Host-Microbe Interface. *mSystems* **2019**, *4* (4), 00125–19.
- (21) Mimeo, M.; et al. An ingestible bacterial-electronic system to monitor gastrointestinal health. *Science* **2018**, *360*, 915–918.
- (22) Sun, Y.; Zhong, X.; Dennis, A. M. Minimizing near-infrared autofluorescence in preclinical imaging with diet and wavelength selection. *J. Biomed. Opt.* **2023**, *28* (9), 094805.
- (23) Sarrion-Perdigones, A.; Chang, L.; Gonzalez, Y.; Gallego-Flores, T.; Young, D. W.; Venken, K. J. T.; et al. Examining multiple cellular pathways at once using multiplex hexuple luciferase assaying. *Nat. Commun.* **2019**, *10* (1), 5710.
- (24) Kreth, J.; Abdelrahman, Y. M.; Merritt, J. Multiplex Imaging of Polymicrobial Communities-Murine Models to Study Oral Microbiome Interactions. *Methods Mol. Biol.* **2020**, *2081*, 107–126.
- (25) Daniel, C.; Poiret, S.; Dennin, V.; Boutillier, D.; Pot, B. Bioluminescence imaging study of spatial and temporal persistence of *Lactobacillus plantarum* and *Lactococcus lactis* in living mice. *Appl. Environ. Microbiol.* **2013**, *79*, 1086–1094.
- (26) Choudhary, R.; Mahadevan, R. Toward a systematic design of smart probiotics. *Curr. Opin. Biotechnol.* **2020**, *64*, 199–209.
- (27) Zheng, L.; Kelly, C. J.; Colgan, S. P. Physiologic hypoxia and oxygen homeostasis in the healthy intestine. A Review in the Theme: Cellular Responses to Hypoxia. *Am. J. Physiol. Cell Physiol.* **2015**, *309* (6), C350–C360.
- (28) Rigottier-Gois, L. Dysbiosis in inflammatory bowel diseases: the oxygen hypothesis microbe-microbe and microbe-host interactions. *Isme J.* **2013**, *7*, 1256–1261.
- (29) Shimizu, T.; et al. Sulfide-responsive transcriptional repressor SqrR functions as a master regulator of sulfide-dependent photosynthesis. *Proc. Natl. Acad. Sci. U. S. A.* **2017**, *114*, 2355–2360.
- (30) Sonnenborn, U.; Schulze, J. The non-pathogenic *Escherichia coli* strain Nissle 1917 – features of a versatile probiotic. *Microb. Ecol. Health Dis.* **2009**, *21*, 122–158.
- (31) Carlson, J. C.; Badran, A. H.; Guggiana-Nilo, D. A.; Liu, D. R. Negative selection and stringency modulation in phage-assisted continuous evolution. *Nat. Chem. Biol.* **2014**, *10*, 216.
- (32) Ross, W.; Aiyar, S. E.; Salomon, J.; Gourse, R. L. *Escherichia coli* Promoters with UP Elements of Different Strengths: Modular Structure of Bacterial Promoters. *J. Bacteriol.* **1998**, *180*, 5375–5383.
- (33) Presnell, K. V.; Flexer-Harrison, M.; Alper, H. S. Design and synthesis of synthetic UP elements for modulation of gene expression in *Escherichia coli*. *Synth. Syst. Biotechnol.* **2019**, *4*, 99–106.
- (34) Salis, H. M.; Mirsky, E. A.; Voigt, C. A. Automated design of synthetic ribosome binding sites to control protein expression. *Nature Biotechnol.* **2009**, *27*, 946–950.
- (35) Bichara, M.; Wagner, J.; Lambert, I. B. Mechanisms of tandem repeat instability in bacteria. *Mutat. Res.* **2006**, *598*, 144–163.
- (36) Kelly, D. P.; Chambers, L. A.; Trudinger, P. A. Handbuch Der Anorganischen Chemie. *Bull. Chem. Soc. Jpn.* **1952**, *2*.
- (37) Wang, T.; Ran, M.; Li, X.; Liu, Y.; Xin, Y.; Liu, H.; Liu, H.; Xia, Y.; Xun, L.; et al. The Pathway of Sulfide Oxidation to Octasulfur Globules in the Cytoplasm of Aerobic Bacteria. *Appl. Environ. Microbiol.* **2022**, *88* (3), No. e01941-21.
- (38) Knoke, L. R.; et al. The role of glutathione in periplasmic redox homeostasis and oxidative protein folding in *Escherichia coli*. *Redox Biol.* **2023**, *64*, 102800.
- (39) Yan, Z.; et al. Effects of His-Tag Length on the Soluble Expression and Selective Immobilization of D-Amino Acid Oxidase from *Trigonopsis variabilis*: A Preliminary Study. *Processes* **2023**, *11*, 1588.
- (40) Reese, A. T.; et al. Antibiotic-induced changes in the microbiota disrupt redox dynamics in the gut. *eLife* **2018**, *7*, No. e35987.
- (41) Winter, S. E.; et al. Host-derived nitrate boosts growth of *E. coli* in the inflamed gut. *Science* **2013**, *339*, 708–711.
- (42) Shibata, H.; Kobayashi, S. Sulfide oxidation in gram-negative bacteria by expression of the sulfide-quinone reductase gene of *Rhodobacter capsulatus* and by electron transport to ubiquinone. *Can. J. Microbiol.* **2011**, *47*, 855–860.
- (43) Cox, G. B.; Newton, N. A.; Gibson, F.; Snoswell, A. M.; Hamilton, J. A. The Function of Ubiquinone in *Escherichia coli*. *Biochem. J.* **1970**, *117*, 551.
- (44) Bekker, M.; et al. Changes in the redox state and composition of the quinone pool of *Escherichia coli* during aerobic batch-culture growth. *Microbiology* **2007**, *153*, 1974–1980.
- (45) Shahak, Y.; et al. Sulfide-quinone and sulfide-cytochrome reduction in *Rhodobacter capsulatus*. *Photosynth. Res.* **1994**, *39*, 175–181.
- (46) Wissenbach, U.; Kröger, A.; Uden, G. The specific functions of menaquinone and demethylmenaquinone in anaerobic respiration with fumarate, dimethylsulfoxide, trimethylamine N-oxide and nitrate by *Escherichia coli*. *Arch. Microbiol.* **1990**, *154*, 60–66.
- (47) Kröger, A.; Biel, S.; Simon, J.; Gross, R.; Uden, G.; Lancaster, C. R. D. Fumarate respiration of *Wolinella succinogenes*: enzymology, energetics and coupling mechanism. *Biochim Biophys Acta.* **2002**, *1553* (1-2), 23–38.
- (48) Zhang, C.; Xing, X. H.; Lou, K. Rapid detection of a gfp-marked *Enterobacter aerogenes* under anaerobic conditions by aerobic fluorescence recovery. *FEMS Microbiol. Lett.* **2005**, *249*, 211–218.
- (49) Hamid, H. A.; Tanaka, A.; Ida, T.; Nishimura, A.; Matsunaga, T.; Fujii, S.; Morita, M.; Sawa, T.; Fukuto, J. M.; Nagy, P.; Tsutsumi, R.; et al. Polysulfide stabilization by tyrosine and hydroxyphenyl-containing derivatives that is important for a reactive sulfur metabolomics analysis. *Redox Biol.* **2019**, *21*, 101096.
- (50) Mishanina, T. V.; Yadav, P. K.; Ballou, D. P.; Banerjee, R. Transient Kinetic Analysis of Hydrogen Sulfide Oxidation Catalyzed by Human Sulfide Quinone Oxidoreductase. *J. Biol. Chem.* **2015**, *290*, 25072–25080.
- (51) Seki, N.; et al. Adverse effects of methylmercury on gut bacteria and accelerated accumulation of mercury in organs due to disruption of gut microbiota. *J. Toxicol. Sci.* **2021**, *46*, 91–97.
- (52) Liu, H.; et al. Synthetic Gene Circuits Enable *Escherichia coli* to Use Endogenous H<sub>2</sub>S as a Signaling Molecule for Quorum Sensing. *ACS Synth. Biol.* **2019**, *8*, 2113–2120.
- (53) De Preter, V.; et al. Decreased mucosal sulfide detoxification is related to an impaired butyrate oxidation in ulcerative colitis. *Inflamm. Bowel Dis.* **2012**, *18*, 2371–2380.
- (54) Giuffrè, A.; Tomé, C. S.; Fernandes, D. G. F.; Zuhra, K.; Vicente, J. B. Hydrogen Sulfide Metabolism and Signaling in the Tumor Microenvironment. *Adv. Exp. Med. Biol.* **2020**, *1219*, 335–353.
- (55) Hayes, J. A.; Lunger, A. W.; Sharma, A. S.; Fernez, M. T.; Carrier, R. L.; Koppes, A. N.; Koppes, R.; Woolston, B. M.; et al. Engineered bacteria titrate hydrogen sulfide and induce concentration-dependent effects on the host in a gut microphysiological system. *Cell Rep.* **2023**, *42* (12), 113481.
- (56) Yamamura, R.; Inoue, K. Y.; Nishino, K.; Yamasaki, S. Intestinal and fecal pH in human health. *Front. Microbiomes* **2023**, *2*, 1192316.
- (57) Cohen, L. J.; Kang, H.-S.; Chu, J.; Huang, Y.-H.; Gordon, E. A.; Reddy, B. V. B.; Ternei, M. A.; Craig, J. W.; Brady, S. F.; et al. Functional metagenomic discovery of bacterial effectors in the human microbiome and isolation of commendamide, a GPCR G2A/132 agonist. *Proc. Natl. Acad. Sci. U. S. A.* **2015**, *112* (35), No. E4825–E4834.
- (58) Woolston, B. M.; Roth, T.; Kohale, I.; Liu, D. R.; Stephanopoulos, G. Development of a formaldehyde biosensor with application to synthetic methylotrophy. *Biotechnol. Bioeng.* **2018**, *115*, 206–215.
- (59) Roth, T. B.; Woolston, B. M.; Stephanopoulos, G.; Liu, D. R. Phage-Assisted Evolution of *Bacillus methanolicus* Methanol Dehydrogenase 2. *ACS Synth. Biol.* **2019**, *8*, 796–806.
- (60) Claassens, N. J.; Siliakus, M. F.; Spaans, S. K.; Creutzburg, S. C. A.; Nijssen, B.; Schaap, P. J.; Quax, T. E. F.; Van Der Oost, J. Improving heterologous membrane protein production in *Escherichia*

coli by combining transcriptional tuning and codon usage algorithms.

*PLoS One* **2017**, *12*, No. e0184355.

(61) Inoue, H.; Nojima, H.; Okayama, H. High efficiency transformation of *Escherichia coli* with plasmids. *Gene* **1990**, *96*, 23–28.

(62) Tan, B.; Jin, S.; Sun, J.; Gu, Z.; Sun, X.; Zhu, Y.; Huo, K.; Cao, Z.; Yang, P.; Xin, X.; Liu, X.; et al. New method for quantification of gasotransmitter hydrogen sulfide in biological matrices by LC-MS/MS OPEN. *Sci. Rep.* **2017**, *7* (1), 46278.